DALTON
FULL PAPER

Calcium fluoride incorporated in soluble organometallics: adduct formation and solution dynamics

Alojz Demsar,*[a] Andrej Pevec,[a] Saša Petriček,[a] Ljubo Golič,[a] Andrej Petrič,[a] Már Björgvinsson[b] and Herbert W. Roesky*[c]

[a] *Faculty of Chemistry and Chemical Technology, University of Ljubljana, Aškerceva 5, SLO-1000 Ljubljana, Slovenia*
[b] *Science Institute, University of Iceland, Dunhaga 3, 107 Reykjavik, Iceland*
[c] *Institut für Anorganische Chemie der Universität, Tammannstrasse 4, D-37077 Göttingen, Germany*

Received 6th August 1998, Accepted 7th October 1998

The recrystallization of $[\{Ti(C_5Me_5)F_3\}_4CaF_2]$ **1** and $[\{Ti(C_5Me_4Et)F_3\}_4CaF_2]$ **2** in the presence of an excess of hmpa (hexamethylphosphoramide) resulted in the formation of $[\{Ti(C_5Me_5)F_3\}_4(CaF_2)(hmpa)]$ **3** and $[\{Ti(C_5Me_4Et)F_3\}_4(CaF_2)(hmpa)]$ **4**, respectively. The adducts **3** and **4** were spectroscopically characterized and the molecular structure of **4** was determined, showing a co-ordination of calcium by eight fluorine atoms from two $[Ti_2(C_5Me_4Et)_2F_7]^-$ moieties and by an oxygen atom of an hmpa ligand. Adduct formation and solution behavior of **2** in different solvents was studied by ^1H and ^{19}F NMR and variable-temperature NMR. A temperature dependent equilibrium between **2** and a solvated form **2**·solv (solv = solvent molecule) is proposed. With increase of the temperature the equilibrium between **2** and **2**·solv was observed to be entropy-shifted to the non-solvated form.

Calcium fluoride is a well known substance and its solid-state chemistry has extensively been studied.[1] However, its solution chemistry has been inaccessible owing to its high lattice energy and, consequently, its low solubility. Furthermore, no molecular adducts of calcium fluoride with donating ligands are known. This is in great contrast to the well known co-ordination chemistry of calcium with oxygen-donating ligands, which play a significant role in many biochemical processes. Different co-ordination chemistry of calcium is expected, however, in a more electronegative environment of co-ordinating fluorine atoms. Thus, in order to extend the co-ordination chemistry of calcium, preparation of soluble compounds with calcium co-ordinated by fluorine-donating ligands is a desirable synthetic target. Furthermore, invaluable additional information can be gained on the solution chemistry of such compounds by the direct ^{19}F NMR measurements of the co-ordinating fluorine environments. In recent years it has been found that organometallic fluorides of d-block elements are capable of forming soluble complexes with main-group metal fluorides.[2] Two examples of capturing *in situ* prepared calcium fluoride have been reported. Calcium fluoride, formed by the reduction of $[Ti(C_5Me_5)F_3]$ with metallic calcium, reacts with the co-ordinatively unsaturated $[Ti(C_5Me_5)F_2]$ giving a soluble paramagnetic complex $[\{Ti(C_5Me_5)F_2\}_6CaF_2]$.[3] Recently we communicated the *in situ* generation of CaF_2 from $CaCl_2$ and $SnMe_3F$, in the presence of $[Ti(C_5Me_4R)F_3]$, yielding the diamagnetic complexes $[\{Ti(C_5Me_4R)F_3\}_4CaF_2]$ (R = Me **1** or Et **2**) (Scheme 1).[4] Each calcium cation in **2** is symmetrically co-ordinated by eight fluorine atoms from two tetradentate $[Ti_2(C_5Me_4Et)_2F_7]^-$ anions. This type of co-ordination is analogous to sandwich-type metal complexes of crown ethers.[5] Furthermore, the Ca–F distances of 2.312 (F_a) and 2.396 Å (F_b) in **2** are comparable to those found in CaF_2[6] (2.366 Å) and $CaZnF_4$ (2.336 and 2.377 Å).[7]

The isolation of the soluble complexes **1** and **2** offers an opportunity to study the co-ordination chemistry of a calcium cation in an all-fluorine environment. Here we report our first study of the adduct formation and solvation behavior of these compounds.

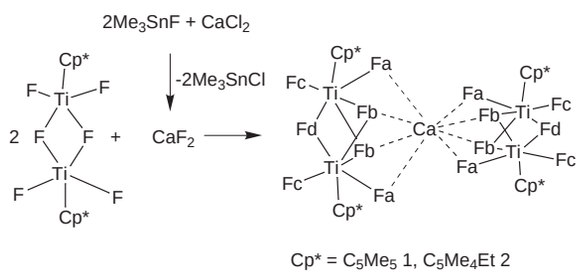

Scheme 1

Experimental

All operations were performed using standard Schlenk techniques under an inert atmosphere of dry nitrogen or argon gas. All solvents were dried over a K/Na alloy and distilled prior to use. The calcium fluoride complexes **1** and **2** were prepared as previously described.[4] Hexamethylphosphoramide [hmpa, $P(NMe_2)_3O$] (Fluka) was used as received. Infrared spectra were recorded on a Perkin-Elmer 1720X spectrometer (FTIR, CsI, Nujol mulls). Melting points were measured using Büchi apparatus and are uncorrected. Elemental analyses were obtained by a Perkin-Elmer 2400 CHN analyzer at University of Ljubljana (Department of Organic Chemistry).

Syntheses

$[\{Ti(C_5Me_5)F_3\}_4(CaF_2)(hmpa)]$ 3. In a Schlenk flask complex **1** (300 mg, 0.289 mmol) was dissolved in 80 mL thf and hmpa (249 mg, 1.16 mmol) added. The clear solution was stirred for 20 h after which thf was removed *in vacuo*. The solid residue was dissolved in thf–hexane (1:1, 60 mL) and the adduct **3** crystallized in the form of yellow intergrown crystals, by slow evaporation of the solvent at reduced pressure. The crystals were washed with *n*-pentane and dried *in vacuo* (250 mg, 70% yield), decomp. 205 °C (Found: C, 44.67; H, 6.42; N, 3.62. $C_{46}H_{78}CaF_{14}N_3OPTi_4$ requires C, 45.37; H, 6.46; N, 3.45%); $\tilde{\nu}_{max}/cm^{-1}$ 1291m, 1199vs, 1100w, 1025w, 981s, 815m, 753m, 634m, 615vs, 561s and 474s (Nujol); ^1H NMR ($CDCl_3$) δ 2.65

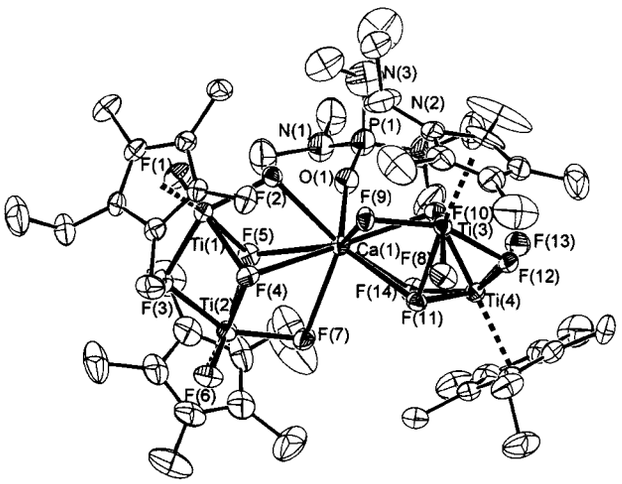

Fig. 1 An ORTEP-like drawing of the adduct $[\{Ti_2(C_5Me_4Et)_2F_7\}_2$-(hmpa)Ca] **4**. Hydrogen atoms are not shown.

[18H, d, *J*(PH) 9 Hz, hmpa], 2.12 and 2.06 (60H, two s, C_5Me_5); ^{19}F NMR ($CDCl_3$) δ 167.7 and 161.9 (4F, two m), 20.9 and 18.9 (4F, two m), −47.4 and −48.4 (2F, two m) and −62.5 (4F, m).

[{Ti(C_5Me_4Et)F_3}$_4$(CaF_2)(hmpa)] 4. In a Schlenk flask complex **2** (274 mg, 0.25 mmol) was dissolved in 30 mL *n*-pentane and hmpa (179 mg, 1.0 mmol) added. The hmpa adduct **4** precipitated as orange prism-shaped crystals when the solvent was slowly evaporated at reduced pressure. The crystals were filtered off and dried *in vacuo* (190 mg, 60% yield), mp 162 °C (Found: C, 46.90; H, 6.80; N, 3.31. $C_{50}H_{86}CaF_{14}N_3OPTi_4$ requires C, 47.15; H, 6.81; N, 3.30%); $\tilde{\nu}_{max}$/cm^{-1} 1291m, 1197vs, 1096m, 1022m, 981s, 803m, 752m, 633m, 616vs, 551s and 466s (Nujol); ^{1}H NMR ($CDCl_3$) δ 2.65 [18H, d, *J*(PH) 9 Hz, hmpa], 2.53 (8H, m, CH_2CH_3), 2.14 and 2.07 [48H, two d, $C_5(CH_3)_4$] and 0.97 (12H, m, CH_2CH_3); ^{19}F NMR ($CDCl_3$) δ 167.6 and 161.7 (4F, two m), 21.5 and 18.6 (4F, two m), −47.5 and −49.1 (2F, two m) and −61.9 (4F, m).

Crystal structure determination of adduct 4

Crystal data. $C_{50}H_{86}CaF_{14}N_3OPTi_4$, M = 1273.4, monoclinic, space group $P2_1/c$ (no. 14), a = 27.768(2), b = 21.176(2), c = 22.747(2) Å, β = 113.000(7)°, U = 12312(2) Å^3, T = 293(2) K, Z = 8, μ(Mo-Kα) = 0.678 mm^{-1}, 31199 reflections measured, 29585 unique (R_{int} = 0.016).

An orange crystal (dimensions: 1.05 × 0.84 × 0.40 mm) from *n*-pentane solution was coated with epoxy glue and used for data collection on an Enraf-Nonius CAD4 diffractometer equipped with graphite-monochromated Mo-Kα radiation (λ = 0.71069 Å). The structure was solved by direct methods and refinement by a full-matrix least-squares method using XTAL 3.2[8] of 1334 parameters on F converged at R = 0.056 and R' = 0.056 using 10624 reflections with $I > 2.5\sigma(I)$.

CCDC reference number 186/1191.

See http://www.rsc.org/suppdata/dt/1998/4043/ for crystallographic files in .cif format.

NMR study

All NMR samples were prepared in C_6D_6, [$^2H_8$]toluene and [$^2H_8$]thf solvents (Aldrich, dried over potassium metal), and $CDCl_3$ (Aldrich, dried over molecular sieves). The ^{1}H and ^{19}F NMR spectra were recorded on a Bruker DPX 300 pulse spectrometer and the respective nuclei referenced to external samples of $SiMe_4$ (^{1}H) and $CFCl_3$ (^{19}F). Variable temperature (222–322 K) spectra were recorded using the variable temperature controller of the spectrometer. The ^{19}F NMR spectra were recorded at 282.4 MHz with 64 k data points and a digital resolution of 2.16 Hz and 141844 Hz spectral width. A 30° flip angle (3.33 μs) was used with a relaxation delay of 0.400 s. The number of scans was 512. The acquisition time was 0.231 s. The sample was allowed to equilibrate for at least 10 min before beginning the spectral accumulation. The sample concentrations were 0.02 M.

Table 1 Selected bond lengths (Å) and angles (°) for one of two different molecules of adduct **4**

Ti(1)···Ti(2)	3.081(2)	Ti(2)–F(7)	1.896(4)
Ti(3)···Ti(4)	3.085(2)	Ca(1)–F(2)	2.424(4)
Ti(1)···Ca(1)	3.469(2)	Ca(1)–F(4)	2.666(4)
Ti(2)···Ca(1)	3.464(1)	Ca(1)–F(5)	2.463(3)
Ti(3)···Ca(1)	3.450(1)	Ca(1)–F(7)	2.423(3)
Ti(4)···Ca(1)	3.466(2)	Ca(1)–F(9)	2.405(3)
Ti(1)–F(1)	1.813(4)	Ca(1)–F(10)	2.478(3)
Ti(1)–F(2)	1.885(3)	Ca(1)–F(11)	2.598(4)
Ti(1)–F(3)	2.019(3)	Ca(1)–F(14)	2.451(4)
Ti(1)–F(4)	2.006(4)	Ca(1)–O(1)	2.295(4)
Ti(1)–F(5)	2.215(4)	O(1)–P(1)	1.471(5)
Ti(2)–F(3)	2.007(4)	P(1)–N(1)	1.617(7)
Ti(2)–F(4)	2.192(3)	P(1)–N(2)	1.619(11)
Ti(2)–F(5)	2.009(3)	P(1)–N(3)	1.675(10)
Ti(2)–F(6)	1.814(4)		
F(1)–Ti(1)–F(2)	96.69(17)	F(2)–Ca(1)–F(5)	64.13(11)
F(1)–Ti(1)–F(3)	90.44(15)	F(2)–Ca(1)–F(7)	114.84(12)
F(1)–Ti(1)–F(4)	146.5(2)	F(2)–Ca(1)–F(9)	75.52(12)
F(1)–Ti(1)–F(5)	79.2(2)	F(2)–Ca(1)–F(10)	112.10(11)
F(2)–Ti(1)–F(3)	145.10(17)	F(2)–Ca(1)–F(11)	136.16(11)
F(2)–Ti(1)–F(4)	81.52(14)	F(2)–Ca(1)–F(14)	158.62(12)
F(2)–Ti(1)–F(5)	78.05(13)	F(2)–Ca(1)–O(1)	76.86(18)
F(3)–Ti(1)–F(4)	74.11(13)	Ca(1)–O(1)–P(1)	168.2(4)
F(3)–Ti(1)–F(5)	69.79(13)	O(1)–P(1)–N(1)	109.8(3)
F(4)–Ti(1)–F(5)	67.62(13)	O(1)–P(1)–N(2)	117.1(4)
F(2)–Ca(1)–F(4)	59.70(10)	O(1)–P(1)–N(3)	108.3(4)

Results and discussion

Synthesis and crystal structure

The recrystallization of complexes **1** and **2** from hexane–thf and pentane solutions, respectively, in the presence of an excess of hmpa afforded the adducts $[\{Ti_2(C_5Me_4R)_2F_7\}_2$(hmpa)Ca], (R = Me **3** or Et **4**). The crystal structure of **4** was determined by X-ray single-crystal analysis. There are two independent and slightly different molecules in the structure, one of which is shown in Fig. 1. In each molecule the calcium cation is co-ordinated to eight fluorine atoms from two tetradentate $[Ti_2(C_5Me_4Et)_2F_7]^-$ moieties and an oxygen atom of a hmpa ligand. The geometry of the $[Ti_2(C_5Me_4Et)_2F_7]^-$ moieties is similar to those in **2**,[4] $[PPh_4][\{Ti_2(C_5Me_5)_2F_7\}_2Na]$[9] and $[\{Ti(C_5Me_5)F_3\}_4LiF]$.[10] The Ca–F distances, which range from 2.405 to 2.666 Å (Table 1), are somewhat longer than those in complex **2**. The hmpa ligand is co-ordinated to the calcium cation at normal Ca–O distances[11] with Ca–O–P angles of 168.2(4) and 168.6(4)° for the two independent molecules.

The most interesting aspect of the crystal structure is the distortion of the high S_4 symmetry of complex **2** when a hmpa ligand is co-ordinated to the calcium cation. Thus in **2** the co-ordinating geometry around the calcium cation is dodecahedral and the dihedral angle between the two $[Ti_2(C_5Me_4Et)_2F_7]^-$ moieties is 90° [Fig. 2(a)]. In **4** the two $[Ti_2(C_5Me_4Et)_2F_7]^-$ moieties are rotated relative to each other, giving an approximate tricapped trigonal prism co-ordination geometry around calcium [Fig. 2(b)]. The dihedral angles between the two $[Ti_2(C_5Me_4Et)_2F_7]^-$ moieties in **4** are 54.0(4) and 56.0(4)°, as measured from the F_b–F_b lines of each moiety. In addition to this change in dihedral angle, the co-ordination of hmpa causes the two $[Ti_2(C_5Me_4Et)_2F_7]^-$ moieties to bend away as the angle between their centers and calcium is 152.1(4) and 151.4(4)° for the two molecules. The corresponding angle in **2** is 180°. Further changes are also noticeable such as tilting of the two moieties.

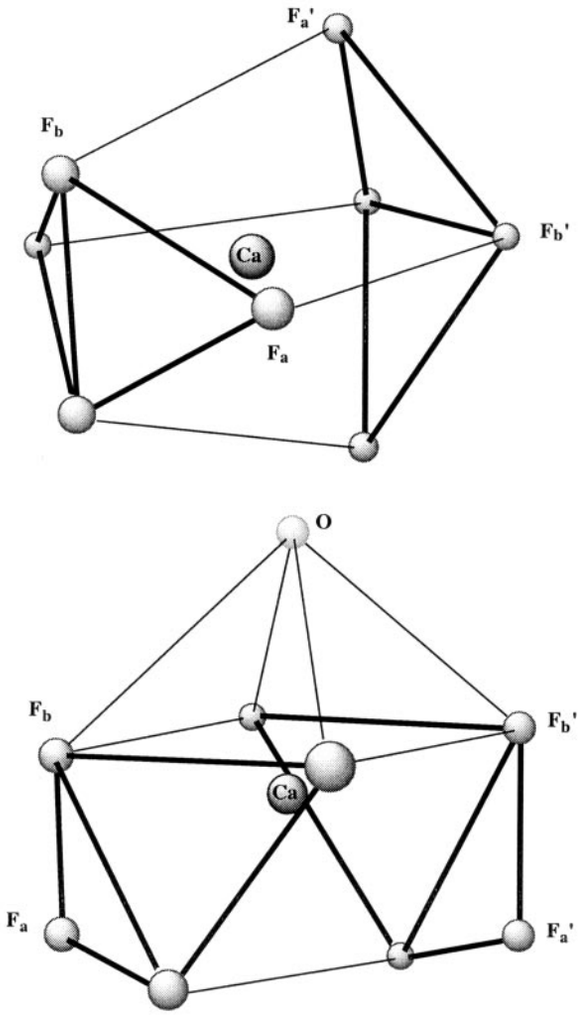

Fig. 2 The dodecahedral (a) (top) and approximate tricapped trigonal prism co-ordination geometry (b) (bottom) of complexes **2** and **4**, respectively. The co-ordinating fluorine atoms (F_a and F_b) of each $[Ti_2(C_5Me_4Et)_2F_7]^-$ moiety are connected by bold lines.

The formation of adducts **3** and **4** demonstrates the Lewis acid character of calcium in the all-fluorine environment of **1** and **2**. Furthermore, the rotation, bending and tilting of the $[Ti_2(C_5Me_4Et)_2F_7]^-$ moieties illustrate the flexibility of these bulky ligands to accommodate the increase in co-ordination number of calcium.

Solution NMR studies of complex 2

When complex **4** is dissolved in toluene it dissociates to a great extent into **2** and hmpa. Furthermore, from previous NMR studies on **2** there was evidence for formation of adducts or solvated species in solution. It was therefore decided to study the solution behaviour of **2** in greater detail by ^1H and ^{19}F NMR spectroscopy.

The ^{19}F and ^1H NMR spectra of complex **2** are solvent- and temperature-dependent. The ^{19}F NMR spectra in $CDCl_3$, $[^2H_8]$toluene, C_6D_6 and C_6D_6–$[^2H_8]$thf solutions are shown in Fig. 3. Four major fluorine resonances, in 4:4:2:4 ratio, are observed in the weakly or non-polar solvents $[^2H_8]$toluene and C_6D_6 [Fig. 3(b) and 3(c)]. The resonances are singlets and consistent with a S_4-coordination symmetry of two $[Ti_2(C_5Me_4Et)_2F_7]^-$ anions around a calcium cation. The resonances have previously been assigned to the following fluorine environments (in order of increasing shielding, see also Scheme 1): terminal (F_c), doubly bridging (F_a), doubly bridging (F_d) and triply bridging (F_b).[4] A new set of 4:4:2:4 fluorine resonances appear, along with the resonances of **2**, when $[^2H_8]$thf is added to a **2**–C_6D_6 solution [Fig. 3(d)]. The intensity

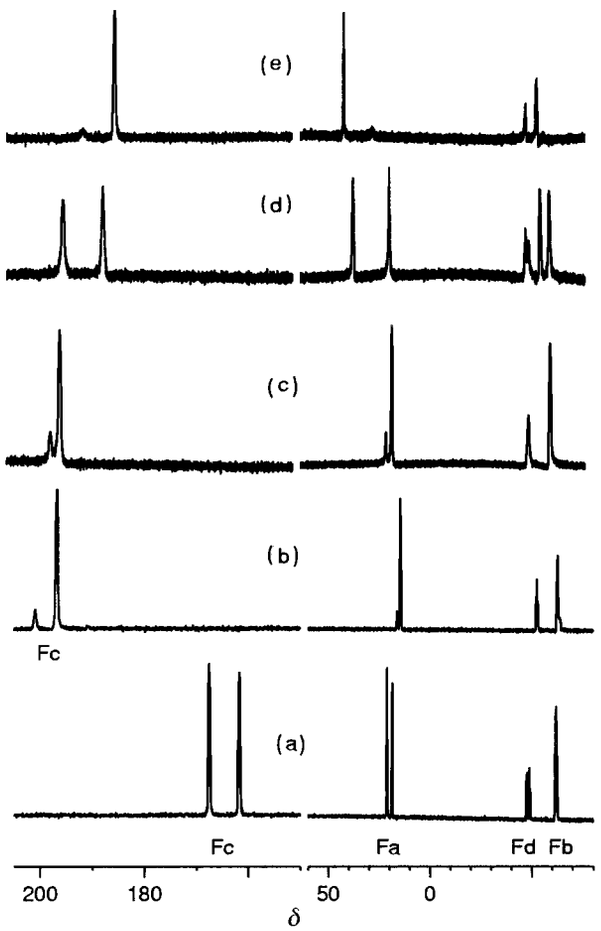

Fig. 3 The ^{19}F NMR spectra of calcium fluoride complex **2** in (a) $CDCl_3$, (b) $[^2H_8]$toluene, (c) C_6D_6, (d) C_6D_6–$[^2H_8]$thf (20:1) and (e) C_6D_6–$[^2H_8]$thf (2:1). See Scheme 1 for labels.

of the new resonances increases with increasing $[^2H_8]$thf concentration and they are the only observed fluorine resonances when the $[^2H_8]$thf:C_6D_6 ratio is 1:2 [Fig. 3(e)]. The new set is assigned to the adduct **2**·$[^2H_8]$thf with a structure similar to that of adduct **4**. The increase of **2**·$[^2H_8]$thf with increasing amount of $[^2H_8]$thf shows that **2** and **2**·$[^2H_8]$thf are in equilibrium in solution. However, the equilibrium is not fast on the NMR timescale as separate resonances are observed for each species.

When complex **4** is dissolved in the polar solvent $CDCl_3$ it dissociates completely as its ^{19}F NMR spectrum is nearly identical with that of a **2**–$CDCl_3$ solution [eqn. (1)]. Interestingly, a

$$\mathbf{4} \xrightarrow{CDCl_3} \mathbf{2} + \text{hmpa} \qquad (1)$$

pair of multiplet resonances are observed in the ^{19}F NMR spectrum of **2**–$CDCl_3$ for each of the F_c, F_a and F_d environments [Figs. 3(a) and 4]. This indicates that there are two separate sets of F_c:F_a:F_d:F_b resonances in the ^{19}F NMR spectrum. The difference in chemical shift for each pair (D_d) decreases in the order: F_c (10), F_a (3), F_d (2 ppm). Owing to this trend, the D_d value for the two F_b enviroments is expected to be small and the two resonances cannot be resolved. The two sets of F_c:F_a:F_d:F_b resonances are assigned to two separate forms of **2**: form **2A** resonating at higher frequency and form **2B** resonating at lower frequency. Variable temperature ^{19}F NMR study of the **2**–$CDCl_3$ solution showed a temperature-dependent equilibrium between **2A** and **2B** [eqn. (2) and Fig. 4]. The

$$\mathbf{2A} \rightleftharpoons \mathbf{2B} \qquad (2)$$

equilibrium constants, $K = C(\mathbf{2B})/C(\mathbf{2A})$, could be calculated from the intensity ratios of the fluorine resonances. The equi-

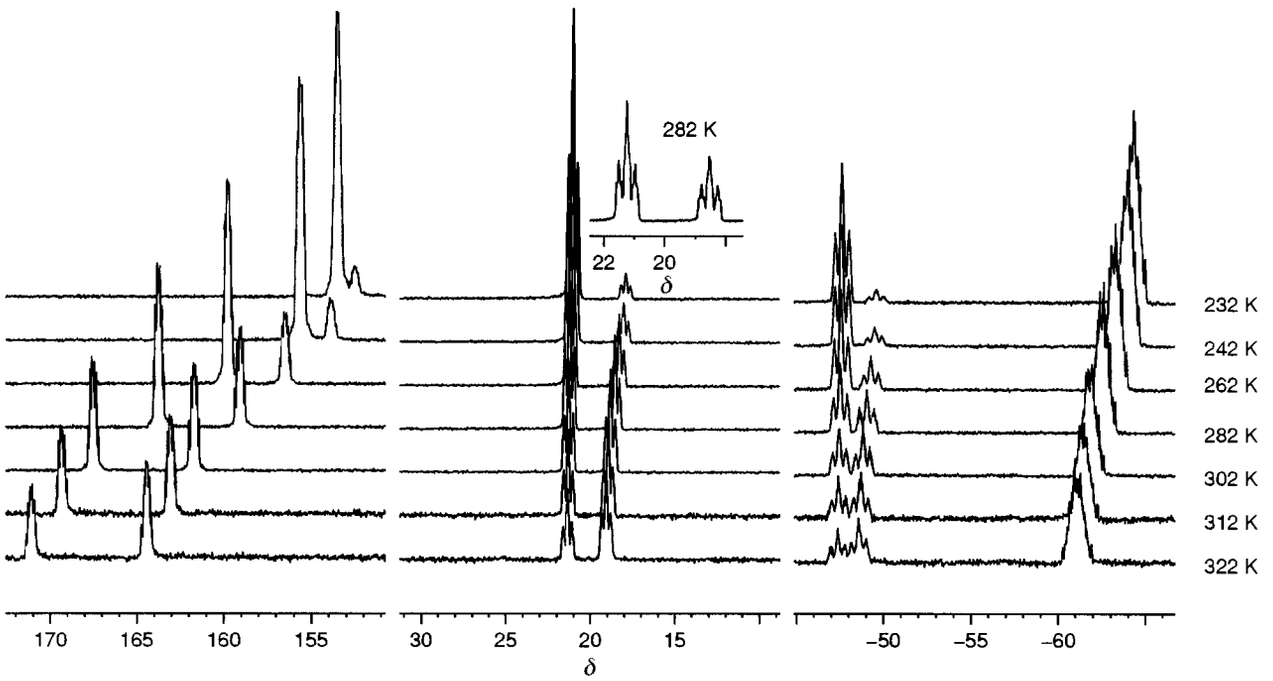

Fig. 4 Variable temperature ^{19}F NMR spectra of calcium fluoride complex **2** in $CDCl_3$.

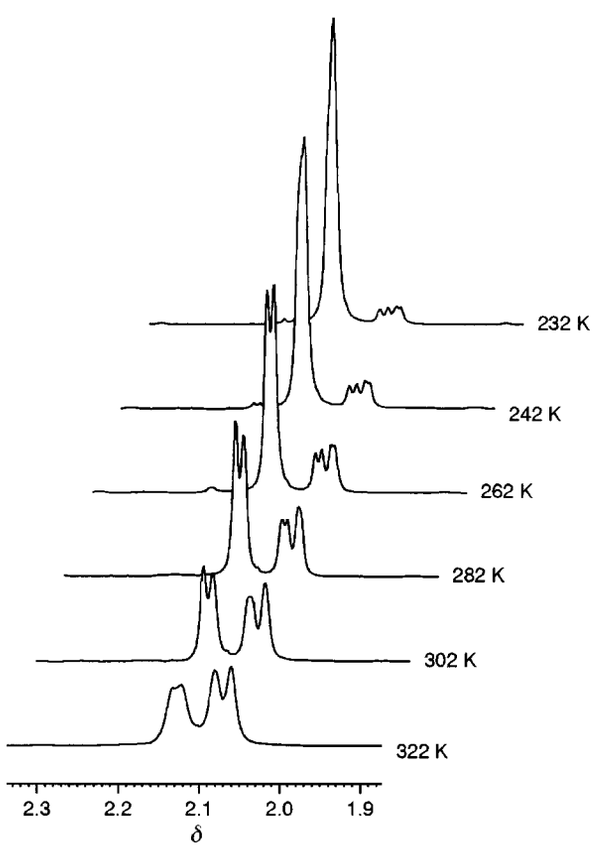

Fig. 5 Variable temperature ^1H NMR spectra (C_5Me_4Et resonances) of calcium fluoride complex **2** in $CDCl_3$.

librium constant changed from 0.09 (232) to 1.44 (322 K). A plot of ln *K versus* 1/*T* gave the following values for the enthalpy and entropy changes of the equilibrium: $\Delta H = +19 \pm 0.2$ kJ mol^{-1} and $\Delta S = +62 \pm 2$ J K^{-1} mol^{-1}. Owing to the lower enthalpy and entropy values of **2A** relative to **2B**, we assign **2A** to be a polar solvated form **2**·solv (solv = solvent molecule) but **2B** to be the S_4-symmetric form of **2**. Furthermore, we suggest the structure **2**·solv to be analogous to that of **4** with the solvent molecule in the co-ordination position of the hmpa

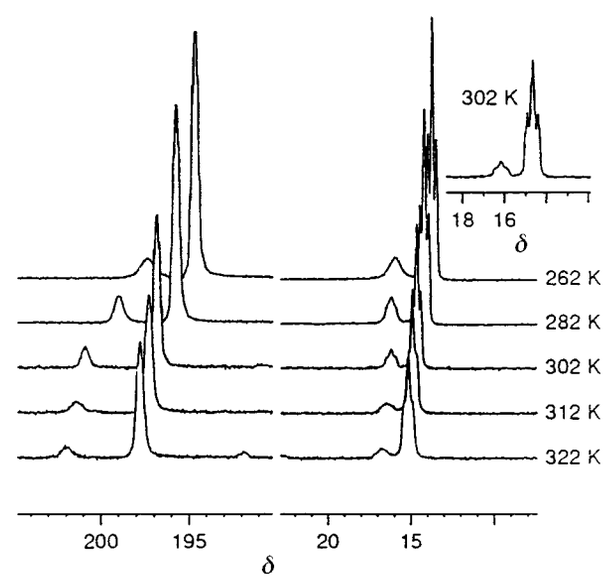

Fig. 6 Variable temperature ^{19}F NMR spectra (F_c and F_a region) of calcium fluoride complex **2** in [$^2H_8$]toluene.

ligand. The lower and, consequent, polar symmetry of **2**·solv and the high heat of solvation should render it the dominant form in polar solvents at lower temperatures. However, at higher temperatures more of it should dissociate into **2** and solvent owing to higher entropy of the dissociated form. The equilibrium of **2A** and **2B** was also observed in variable temperature ^1H NMR spectra (Fig. 5).

Equilibrium (2) was also observed for complex **2** in the weakly polar solvent [$^2H_8$]toluene by variable temperature ^{19}F NMR spectroscopy (Fig. 6). However, the equilibrium is now shifted to the right with the equilibrium constant ranging from 5.7 (246) to 7.3 (322 K). The enthalpy and entropy changes for this equilibrium are $\Delta H = +1.8 \pm 0.6$ kJ mol^{-1} and $\Delta S = +22 \pm 6$ J K^{-1} mol^{-1}. The low values of ΔH and ΔS indicate that a toluene molecule is only weakly bonded in **2**·solv and thus the desolvated non-polar form **2** is the dominating species in weakly or non-polar solvents. Owing to improved signal-to-noise ratio, a small amount of a solvated form **2**·solv is also observed in **2**–C_6D_6 solution [Fig. 3(c)], not

reported previously.[4] The fluorine resonances of **2**·solv in the **2**–C_6D_6 spectrum disappear after addition of a small amount of thf (molar ratio **2**:thf = 1:2.5), resulting in a spectrum similar to that shown in Fig. 3(d) with **2**:**2**·thf ratio of 1:0.3. The resonances of terminal fluorine atoms in **2**–$CDCl_3$ solution are shifted for about 30 ppm to lower frequencies in comparison with C_6D_6 or [$^2H_8$]toluene solutions, similarly to those observed for [{Ti(C_5Me_5)F_3}$_4$LiF].[10]

Equilibrium (2) is not fast on the NMR timescale as separate resonances are observed for complex **2** and a solvated form **2**·solv. However, there is probably a fast intramolecular rotation of the $[Ti_2(C_5Me_4Et)_2F_7]^-$ anions in **2**·solv as well as in **2**·D adducts (D = donor molecule), which causes the observation of only four F_c:F_a:F_d:F_b fluorine environments. The shape of the fluorine resonances depends on solvent appearing as singlets for **2**·C_6D_6, **2**·[$^2H_8$]toluene and **2**·[$^2H_8$]thf, and as multiplets for **2**·$CDCl_3$ (quintet for F_c, triplet of multiplets for F_a and F_d and multiplet for F_b, see Fig. 4). At present the mechanism of the intramolecular rotation is not known.

Conclusion

The isolation of adducts **3** and **4** and the crystal structure of **4** demonstrate the Lewis acid character of complexes **1** and **2**, and the flexibility of the tetradentate $[Ti_2(C_5Me_4R)_2F_7]^-$ ligands in co-ordinating to calcium. Thus the $[Ti_2(C_5Me_4R)_2F_7]^-$ unit is structurally similar to $[Zr_2(OPr^i)_9]^-$, a polydentate ligand, which is regarded as a substitute for cyclopentadienyl ligands.[12] The observation of a separate solvated form **2**·solv, even with weakly or non-polar solvent molecules, underlines further the Lewis acid character of calcium in the all-fluorine environment of **2**. In addition, the monitoring of a equilibrium between **2** and **2**·solv by variable temperature NMR spectroscopy can give important insight into the relative stability of these species. Invaluable information can, therefore, be obtained on the Lewis acid character of **1** and **2** by direct observation of the relevant species in solution by NMR spectroscopy.

Acknowledgements

This work was supported by the Ministry of Science and Technology Republic of Slovenia and the Deutsche Forschungsgemeinschaft.

References

1 G. J. Miller, in *Encyclopedia of Inorganic Chemistry*, ed. R. B. King, Wiley, Chichester, 1994, vol. 3, p. 1343 and refs. therein.
2 E. F. Murphy, R. Murugavel and H. W. Roesky, *Chem. Rev.*, 1997, **97**, 3425.
3 F.-Q. Liu, D. Stalke and H. W. Roesky, *Angew. Chem.*, 1995, **107**, 2004; *Angew. Chem., Int. Ed. Engl.*, 1995, **34**, 1872.
4 A. Pevec, A. Demsar, V. Gramlich, S. Petricek and H. W. Roesky, *J. Chem. Soc., Dalton Trans.*, 1997, 2215.
5 E. Mason and H. A. Eick, *Acta Crystallogr., Sect. B*, 1982, **38**, 1821.
6 B. G. Hyde and S. Andersson, *Inorganic Crystal Structures*, Wiley, New York, 1989, p. 187.
7 H. G. von Schnering, D. Vu and K. Peters, *Z. Kristallogr.*, 1983, **165**, 305.
8 *XTAL 3.2 Reference Manual*, eds. S. R. Hall, H. D. Flack and J. M. Steward, Universities of Western Australia, Geneve and Maryland, 1992.
9 H. W. Roesky, M. Sotoodeh and M. Noltemeyer, *Angew. Chem.*, 1992, **104**, 869; *Angew. Chem., Int. Ed. Engl.*, 1992, **31**, 864.
10 A. Demsar, A. Pevec, L. Golič, S. Petriček, A. Petrič and H. W. Roesky, *Chem. Commun.*, 1998, 1029.
11 K. G. Caulton, M. H. Chisholm, S. R. Drake, K. Folting, J. C. Huffman and W. E. Streib, *Inorg. Chem.*, 1993, **32**, 1970; M. G. Davidson, P. R. Raithby, R. Snaith, D. Stalke and D. S. Wright, *Angew. Chem.*, 1991, **103**, 1696; *Angew. Chem., Int. Ed. Engl.*, 1991, **30**, 1648; Z. Hou, X. Jia, M. Hoshino and Y. Wakatsuki, *Angew. Chem.*, 1997, **109**, 1348; *Angew. Chem., Int. Ed. Engl.*, 1997, **36**, 1292.
12 W. J. Evans, M. A. Greci, M. A. Ansari and J. W. Ziller, *J. Chem. Soc., Dalton Trans.*, 1997, 4503.

Paper 8/06209I